

Comparative Study of Multielectron Ionization of Alkyl Halides Induced by Picosecond Laser Irradiation

S. Kaziannis and C. Kosmidis*

Department of Physics, University of Ioannina, 45110 Ioannina, Greece

Received: December 4, 2006; In Final Form: February 5, 2007

The interaction of C_2H_5X , $1-C_3H_7X$, $1-C_4H_9X$, where $X = I, Br, Cl$, with strong (1×10^{13} – 1.2×10^{14} W/cm²) 35 ps laser pulses at 1064 nm is studied by means of time-of-flight mass spectrometry. The multielectron ionization following the C–X bond elongation has been verified for the studied molecules. By combination of the intensity dependence of the ion yields, the estimated kinetic energies of the released fragment ions, and their angular distributions, we have identified the different dissociation channels of the transient multiply charged parent ions. From the dependence on the laser intensity of the ratio of the doubly charged halogen ions to the singly charged ones, it is concluded that the molecular coupling with the laser field increases with the molecular size.

Introduction

Over the last 10 years there has been an increasing concern about the response of polyatomic molecules with strong IR laser fields and particularly the dependence of the ionization/dissociation probabilities on the molecular size. The complexity of the large molecular systems prohibits the detailed calculations of the ionization rates, especially under irradiation intensities for which the equivalent electric field strength is ~ 1 – 10 V Å⁻¹. In that case, the laser field is strong enough to sufficiently distort the electrostatic potential of the molecule, making impossible the theoretical treatment of the laser–molecule interaction without the use of approximations.

Among the first attempts for the theoretical description of the laser–molecule interaction was to apply the tunneling ionization model that Keldysh proposed for the interaction of strong laser fields with atoms.¹ According to the Keldysh approach, the atomic ionization is a tunneling process of the most weakly bound electron through a barrier determined by the superposition of the zero-range Coulombic field of the core and that of the laser field. Although this theory was proven quite successful for the case of rare gas atoms, it failed to predict some of the experimental observations for the interaction of molecules with moderate/strong laser fields.

Particularly, a series of publications by Levis et al.^{2–5} on the ionization/dissociation processes of various organic molecules during their interaction with moderate IR laser fields showed that both of the above processes are enhanced for the larger molecules. This conclusion resulted from the comparison of the total ionic signal for the various molecules under the same irradiation intensities. In addition to the experimental work, the same group proposed a model for the interpretation of their results, known as the structure-based tunneling ionization model (SBTI). In fact, this model is a revision of the Keldysh tunneling theory, where the zero-range potential was replaced by a potential of an effective length determined by the molecular parameters.

However, later experiments by Hankin et al.⁶ on a large number of polyatomic molecules suggested, somehow, the

opposite effect of the molecular size on the ionization rates. In particular, the intensity thresholds for efficient ionization of large polyatomic molecules were found higher than the ones for atoms of similar ionization energies. The same trend was also confirmed by Lezius et al.,⁷ in his comparative work on a series of organic molecules. Moreover, the numerical simulation described in the same publication suggested that the decrease of the ionization rate for molecules of increasing size stems from multielectron excitation phenomena, i.e., under the same irradiation conditions the probability of multiple electrons being affected by the laser field increases with the molecular size. Furthermore, the increased polarizability of the large molecules facilitates the displacement of the distribution of the excited electrons toward the lowered part of the molecular potential well. Thus, an additional repulsion builds up at the end of the potential barrier reducing, in that way, the possibility of tunneling of the most weakly bound electron through the potential well. This particular approach varies essentially from the one introduced by Keldysh and the early works by Levis' group, according to which the laser–molecule interaction is a single-electron excitation. The importance of the multielectron excitation phenomena in the ionization/fragmentation processes of large organic molecules, under strong laser irradiation, has also been the subject of later experimental and theoretical work.^{8–10}

Nevertheless, all of the experimental results mentioned above concern the interaction of organic polyatomic molecules with laser pulses of moderate intensities $\sim 10^{13}$ – 10^{14} W/cm² and pulse durations varying in the range of 40–120 fs. The relatively short pulse durations and the low laser intensities were used by the authors mentioned above to minimize the contribution of the enhanced multielectron ionization phenomenon, which takes place at well-defined internuclear distances (R_{cr}) larger than the equilibrium ones. This phenomenon has been studied extensively for small and especially diatomic molecules,¹¹ and the experimental results can be adequately interpreted by the theoretical models of Seideman and Posthumus.^{11–14}

On the other hand, there have been only few reports on the relative ionization probabilities for molecules of varying size under laser irradiation conditions that favor the enhanced multielectron ionization. Especially, the work of Hering et al.

* To whom correspondence should be addressed. E-mail address: kkosmid@uoi.gr. Fax: +30-26510-98695.

concerned the relative production of multicharged atomic ions during the interaction of small molecules with strong laser fields $\sim 10^{14}$ – 10^{16} W/cm² and relatively longer (160 fs) pulse duration.¹⁵ One of the main conclusions of their work is that there is insignificant difference in the multicharged ion production efficiency for diatomic and triatomic molecules, consisting of the same atoms. This result was also found valid for the production of multiply charged carbon ions coming from the C₂H₄ and C₃H₄ molecules.¹⁶

On the contrary, the interaction of some alkyl iodides with strong $\sim 10^{14}$ – 10^{16} W/cm² laser fields of 50 fs pulse duration, studied by our group,¹⁷ clearly showed an increase of the ionization rates for the larger molecules under study in comparison to the smaller ones. In this case, the increased ionization rates of the longer molecules were verified by the lower-intensity thresholds for the detection of I^{*n*+}, *n* = 1–7. fragment ions, in comparison to the corresponding values for the smaller alkyl iodides. However, the corresponding study of the ionization/dissociation processes of the same alkyl iodides with picosecond laser pulses did not show a clear trend for the intensity thresholds of the I^{*n*+}, *n* = 1–7 fragment ions.¹⁸ To the best of our knowledge, this is the only available comparative study of the ionization process of organic polyatomic molecules of approximately the same vertical ionization potential under strong picosecond laser irradiation.

In the present work, we attempt to expand the study to different molecular species. Moreover, to improve the accuracy of our measurements, we modified the experimental setup with the view of collecting ions that are generated within the hottest part of the focused laser beam. The molecules chosen for the present study are also members of the alkyl halides group, with increasing size for the molecular chain and therefore increasing polarizability. In particular, the molecules under study are the following: C₂H₅X, 1-C₃H₇X and 1-C₄H₉X, where X = I, Br, Cl.

Experimental Details

The Nd–YAG picosecond laser system (Quantel YG-901C) used produces 35 ps pulses at 1064 nm, with 80 mJ energy per pulse at a repetition rate of 10 Hz.

A time-of-flight mass spectrometer based on a Wiley–McLaren design, with a 1.4-m-long field-free tube, was used for ion analysis. The ions produced in the molecule–laser interaction region were accelerated by a dual-stage electrostatic field under variable potential (0–3000 V). An electrode with a 1-mm pinhole separated the two field stages. Furthermore, to increase the angular and mass resolution of the spectrometer, another 1-mm pinhole at a distance of 12 cm from the acceleration region has been added. The electronic signal was recorded with an Agilent 54830B (600 MHz, 4Gs/s) digital oscilloscope. The mass resolution was typically 700 at 100 Da.

The background pressure of the system was below 10^{–7} Torr, while the molecular vapor was allowed to expand through a needle valve into the interaction region. During the experiments the pressure in the chamber was kept below 3 × 10^{–7} Torr to ensure that no space-charge effects were perturbing the mass spectrum measurements. The studied alkyl halides were purchased from Fluka and had purity better than 99.5%, while they were used after several repeated freeze–thaw–degassing cycles under vacuum.

The laser light was focused with a 250-mm focal length lens at about 1 cm from the repeller electrode. Taking into account the Gaussian profile of the 1064 nm laser beam the diameter of the beam at the focus is estimated to be 33 μm, while the

corresponding Rayleigh range is estimated to be 32 mm, which is significantly longer than the width of the spectrometer's pinholes, mentioned above. Thus, the combination of the particular focal length lens and the small diameter pinholes ensures that the ionic signal collected is produced only in the center portion of the total focal volume. Furthermore, the polarization of the laser light was controlled with a Brewster angle polarizer and was rotated by using a half-wavelength plate. The intensities attained at the focus were also checked through comparison with the intensities needed to produce multiply charged Argon ions.¹⁹

Results and Discussion

In Figures 1–3, the mass spectra of some alkyl halides, (C₂H₅X, 1-C₃H₇X, 1-C₄H₉X, X = I, Br, Cl) induced by 35 ps laser irradiation at the intensity of $\sim 1.0 \times 10^{14}$ W/cm² are presented. The laser polarization vector for all cases was set parallel to the time-of-flight axis, while the vertical axis of the mass spectra has been divided by the height of the X⁺ ion peak to facilitate the comparison of the relative abundance of the recorded atomic and molecular fragment ions.

One common feature observed in the mass spectra of these molecules is that the highest observed charge state of the carbon atomic ions is C²⁺. Moreover, the charge states that have been observed for the halogen atomic ions are independent of the size of the molecular chain. For all the alkyl bromides and alkyl chlorides, the singly and doubly charged halogen ions have been recorded, while for the case of alkyl iodides, at the same laser intensity, up to triply charged halogen ions have been detected (I³⁺). The above observations imply that the ionization rate is not dramatically dependent on the size of the molecular chain. Thus, at first sight, this result is in accordance with those reported by Hering et al. for the multiple ionization of diatomic and triatomic molecules consisting of the same kind of atoms¹⁵ and with our previous work on alkyl iodides under strong picosecond laser irradiation.¹⁸

On the other hand, the comparison of the mass spectra for molecules of increasing size clearly implies that the fragmentation probability is enhanced as the size of the alkyl chain increases. For example, it is easy to observe that the relative abundance of small fragments, such as H⁺ and C⁺, increase along with the size of the molecules and finally become the prominent peaks for 1-C₄H₉X. At the same time, the intensity of the parent molecular ion P⁺ peak and that of the larger molecular fragments ([P–I]⁺) decrease. This tendency for increasing dissociation of molecular ions with increasing size has also been reported for a series of molecules in the past, and different interpretations have been proposed.^{2,20} Moreover, the ionization–fragmentation processes of cyclic polyatomic molecules, under strong femtosecond laser irradiation, and, especially, the production of multiply charged intact ions were also found to be dependent on other molecular parameters, such as the aromaticity and the nature of the highest occupied molecular orbital.²¹ Finally, the possibility for the above processes to be critically affected by resonance of the laser wavelengths with the absorption spectra of the molecular ions has also been investigated with contradictory results.^{22–25}

However, the differences in the fragmentation processes observed in the present study cannot unambiguously be attributed to one of the various interpretations mentioned above. It is well established, for the interaction of alkyl iodides with strong picosecond laser irradiation that the ionization/dissociation processes can be partly attributed to the contribution of the well-known ladder-switching mechanism.^{18,26} Therefore, the

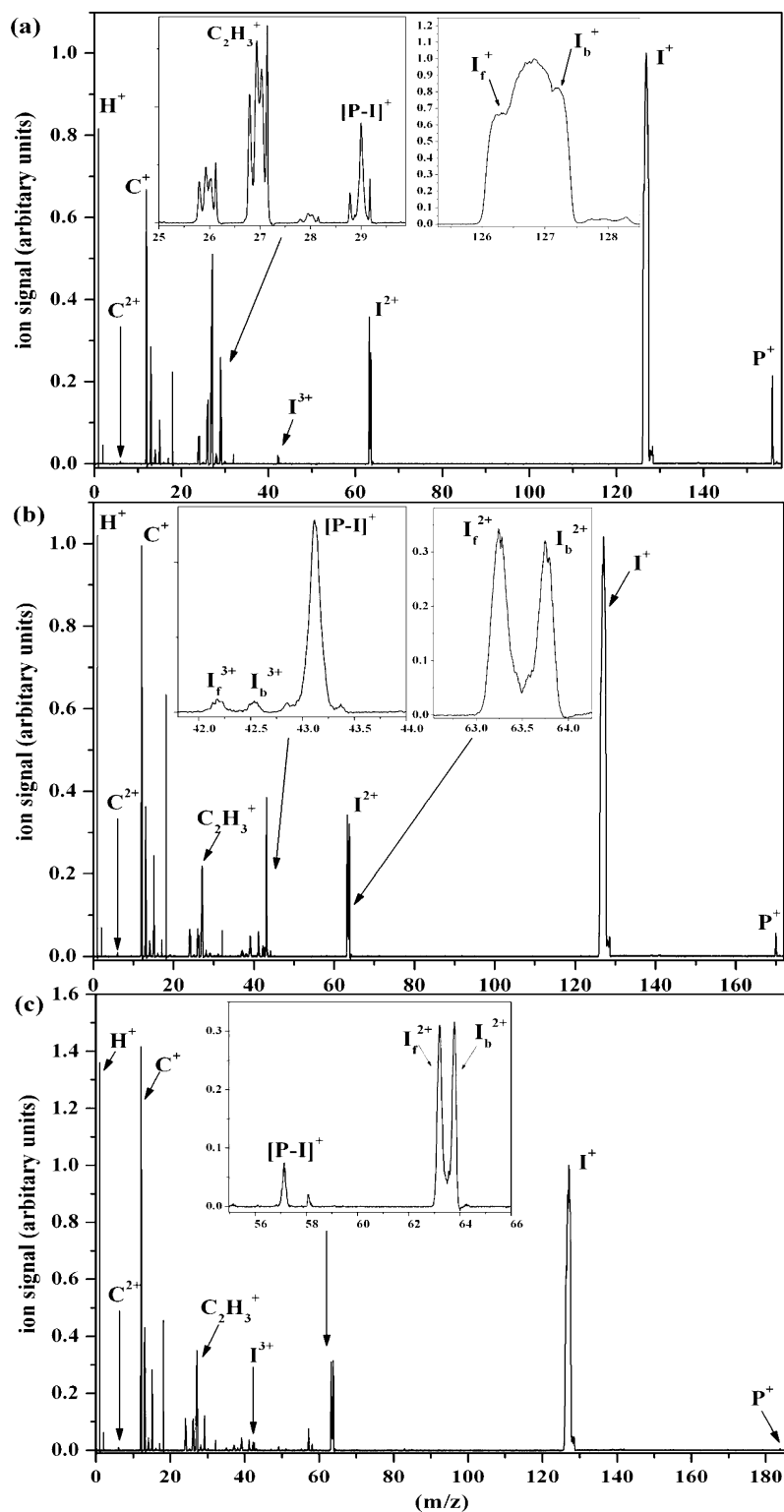


Figure 1. Mass spectra of the alkyl iodides under study recorded at the intensity of 1.0×10^{14} W/cm². The a, b, and c mass spectra correspond to C₂H₅I, 1-C₃H₇I, and 1-C₄H₉I, respectively.

relative abundance of the recorded H⁺, C⁺, and C²⁺ fragment ions and the total ion signal as well cannot be used as a safe criterion for the dependence of the laser–molecule coupling on the molecular size. As an alternative, we choose to focus on the relative abundance of halogen ions and their intensity thresholds, since these ions are produced mainly from the direct dissociation of parent molecular ions, through the rupture of the C–X molecular bond. In this case, the only additional process contributing to the production of halogen fragment ions

is the possibility for them to be further ionized, within the same laser pulse duration.

The Alkyl Iodides. The ionization/dissociation processes of alkyl iodides under strong picosecond and femtosecond laser pulses have been the subject of extensive experimental studies presented recently.^{17,18,26,27} Under strong picosecond laser irradiation at 1064 nm, there is strong contribution from field ionization processes in the molecular ionization along with MPI that is taking place, at least, at the spatial and temporal wings

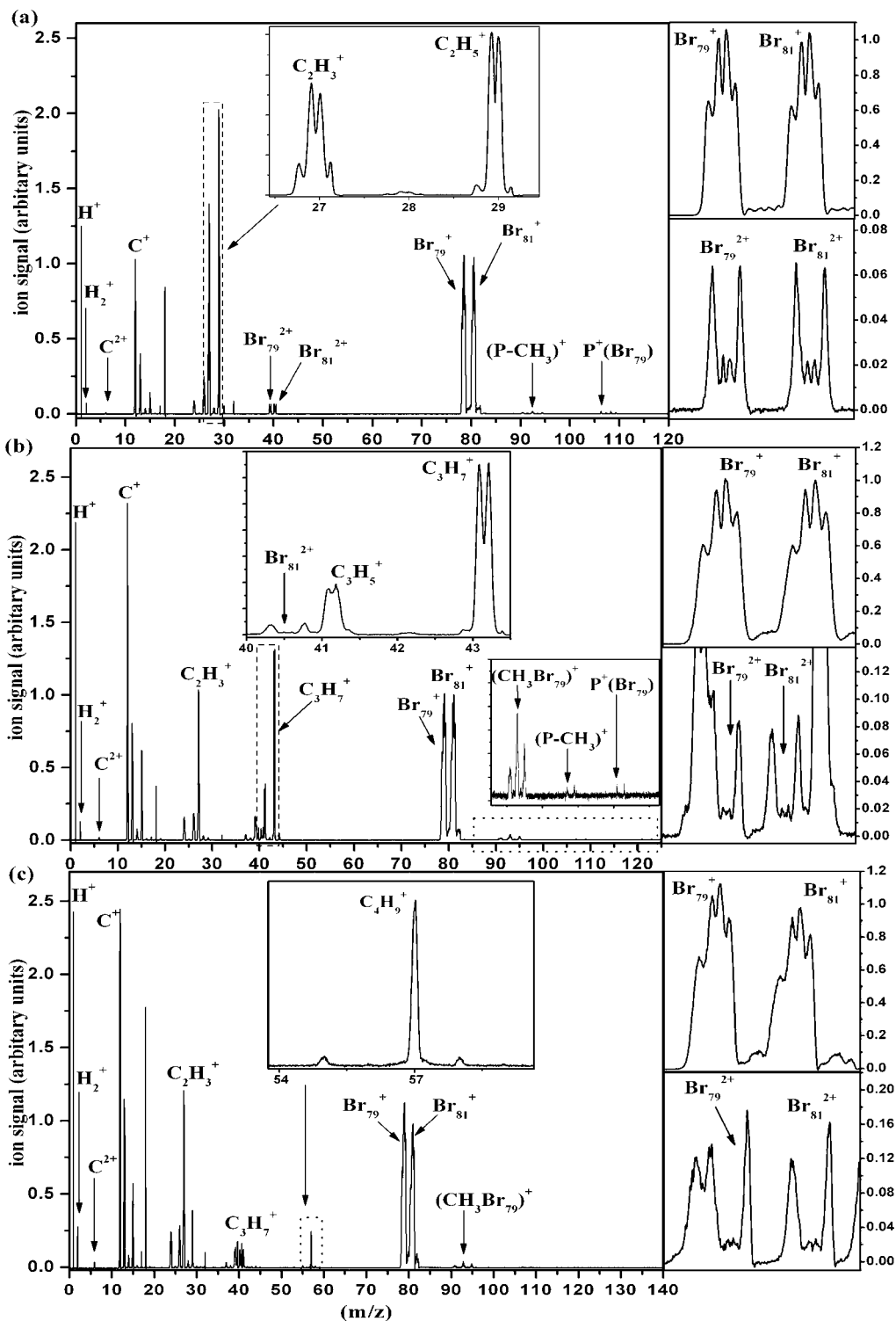


Figure 2. Mass spectra of the alkyl bromides under study recorded at the intensity of 1.0×10^{14} W/cm². The a, b, and c mass spectra correspond to C₂H₅Br, 1-C₃H₇Br, and 1-C₄H₉Br, respectively.

of the focused laser beam. The relative abundance of the molecular ions in the mass spectra of the alkyl iodides, under study, has been attributed to the well-known competitive “ladder switching” and “ladder climbing” ionization/dissociation mechanisms. The intermediate dissociative A state (~ 4.7 eV) can be reached by four photon absorption at 1064 nm, leading to the cleavage of the C–I bond, within a time scale of a few hundreds of femtoseconds, which is much shorter than the pulse duration of the picosecond laser pulses.

Furthermore, the contribution from Coulomb explosion of multiply charged molecular ions ($[P^{n+}]$, $n = 2, 3$) in the

production of I^+ and I^{2+} , has been verified by the split peaks profile of these ions, along with their estimated kinetic energies. The Coulomb explosion process leads to the production of the I^+ and I^{2+} fragments. As far as, the higher multiply charged ions I^{n+} , ($n \geq 3$) are concerned they were produced by further ionization of the molecular fragments, through field ionization processes.

In the present study, similar complex peak profiles are observed for the I^{n+} , ($n = 1 - 3$) ions, as it is depicted in the insets to the mass spectra of Figure 1, for the case of I^+ and I^{2+} ions. Following the same procedure, the time-of-flight separation

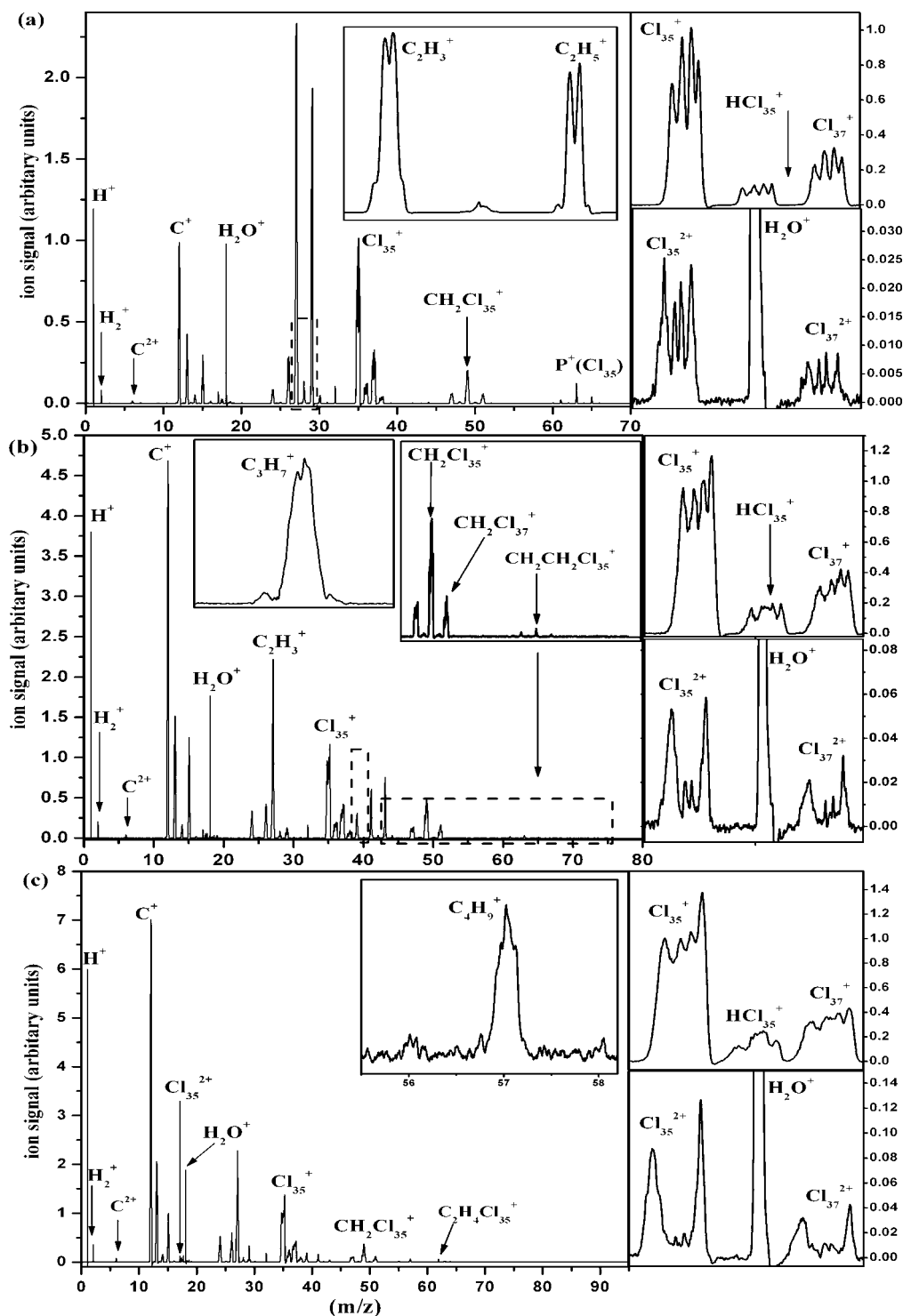


Figure 3. Mass spectra of the alkyl chlorides under study recorded at the intensity of 1.0×10^{14} W/cm². The a, b, and c mass spectra correspond to C₂H₅Cl, 1-C₃H₇Cl, and 1-C₄H₉Cl, respectively.

between the two peak (backward and forward) components is used in order to estimate the kinetic energies of the P^{n+} , which are in reasonable agreement with those reported for 1-C₃H₇I and 1-C₄H₉I in ref 18. However, the C₂H₅I was not included in the molecules studied in our previous report. Thus, the experimental results for this molecule are discussed in the following.

The parent ion peak, C₂H₅I⁺, has been recorded along with various molecular and atomic fragment ions. The peak profile of the [P-I]⁺ fragment consists of one middle component coming from the photodissociation of the neutral and/or the

singly charged parent ion and a pair of backward and forward components, which correspond to an average kinetic energy of $E_{\text{kin}}[\text{C}_2\text{H}_5^+] = 2.8 \pm 0.2$ eV. The kinetic energy values were estimated by taking into account the time difference between the backward and forward components (Δt (nsec)) and using the following equation

$$E \text{ (eV)} = 9.65 \times 10^{-7} \frac{n^2 \Delta t^2 F^2}{8m}, \quad (1)$$

where n is the charge state, F (V/cm) the extraction, and m the

TABLE 1: Intensity Thresholds for the Production of the I^{n+} , $n = 1-3$, Fragments under Picosecond Laser Irradiation

intensity thresholds (10^{13} W/cm 2)	I^{3+}	I^{2+}	I^{+}
C_2H_5I	3.3 ± 0.2	2.7 ± 0.2	$\leq 1.6 \times 10^{13}$
$1-C_3H_7I$	3.1 ± 0.2	2.3 ± 0.2	
$1-C_4H_9I$	3.1 ± 0.2	2.3 ± 0.2	

ion mass. These two components are attributed to the same dissociation channel, due to their common dependence on the angle between the laser polarization and the time-of-flight axis. In the same way, different dissociation channels are discriminated in the complicated peak profile of the I^+ . The I^+_f and I^+_b components, depicted in the inset of the C_2H_5I mass spectra, are generated from a common dissociation channel that gives rise to ions with a kinetic energy of $E_{kin}I^+ = 0.70 \pm 0.08$ eV, while the middle component can be attributed to the photodissociation of a neutral or singly charged molecular ion. Moreover, the values of the E_{kin} of the I^+_f and I^+_b components and that of $C_2H_5^+$ are found to be in accordance with the conservation of momentum, provided that they are produced from the dissociation of a common precursor, which in this particular case is the unstable $[P^{2+}]$. An approximate estimation for the critical length of the C–I bond can be made by using the following equation

$$E_{kin} \text{ (eV)} = 14.4 \frac{Q_1 Q_2}{R_{cr} \text{ (\AA)}} \quad (2)$$

where E_{kin} (eV) is the total kinetic energy of the fragments, Q_1 and Q_2 their corresponding charge states, and R_{cr} (Å) the critical distance between the two charges.²⁸ By application of this relation, the estimated value for the bond length is found to be R_{cr} (Å) = 4.1 ± 0.5 , which is approximately twice the one for the C–I bond in equilibrium (~ 2.1 Å).

In a similar way, the E_{kin} of the I^{2+} (I^{2+_f} , I^{2+_b}) ions is estimated to be $E_{kin}I^{2+} = 1.2 \pm 0.1$ eV. The $E_{kin}I^{2+}$ value is higher than that of I^+ , proving that these fragments are generated from different precursors. Thus, the precursor of I^{2+} should be a transient molecular ion $[P^{n+}]$, with $n \geq 3$. However, the contribution from ionization processes of neutral and/or singly charged iodine ions cannot be excluded. Actually, the contribution of the particular mechanism is verified for the case of I^{3+} by taking into account the fact that the E_{kin} of I^{3+} ($E_{kin}I^{3+} = 1.3 \pm 0.1$ eV) is found to be the same as that of I^{2+} within the range of the experimental errors. Therefore, the experimental results for the interaction of the C_2H_5I with strong IR, picosecond laser irradiation are in complete agreement with the proposed mechanism for the ionization/dissociation processes of alkyl iodides studied earlier, despite the different size of their molecular chain.

The laser intensity threshold for the production of I^+ and I^{2+} ions are found to be the same (within the experimental errors) for all alkyl iodides studied, albeit their actual values are lower than those reported previously, due to the differences in the geometry of the focused beam. The experimental values from the present study are presented in Table 1.

The Alkyl Bromides. Following the same approach with the one proposed for the alkyl iodides the P^+ ions, along with the molecular and atomic fragment ions, which have been recorded in the mass spectra of the corresponding alkyl bromides, could be attributed to the “ladder switching” or the “ladder climbing” mechanism. The dissociation followed by ionization mechanism can be realized through the intermediate dissociative A state, which is optically accessible for these molecules via a four photon absorption at 1064 nm. The four-photon excitation leads

to a final dissociative state, which could be one of the three known excited states 3Q_0 , 3Q_1 , and 1Q_1 , according to Mullikens notation.²⁹ Excitation to the 3Q_0 state is a parallel to the C–Br bond transition leading to the break up of the bond and the production of excited neutral Br^* , while the excitation to the 3Q_1 and 1Q_1 states is a perpendicular transition leading to the production of Br.

The photodissociation dynamics of the alkyl bromides at the level of the A dissociative state has been a subject of recent, extensive experimental work, mainly through resonance-enhanced multiphoton ionization (REMPI) studies for different laser wavelengths.^{30–33} The dissociation of the C–Br bond is a fast process, taking place within a few hundreds of femtoseconds, and for the case of CH_3Br the dissociation time was estimated to be 120 fs.³¹

The small parent ion peaks recorded for the C_2H_5Br and $1-C_3H_7Br$ molecules, depicted in the insets of their mass spectra (Figure 2), and the absence of the parent ion from the mass spectra of $1-C_4H_9Br$ could imply that “ladder switching” is the main ionization/dissociation mechanism. In that case, molecular fragmentation should take place within the laser pulse duration resulting in neutral molecular $[P-Br]$ and atomic Br fragments, which are being ionized by the same laser pulse. As a consequence, the kinetic energies of the atomic Br ions should be the same as those of their neutral precursors, which are determined by the excitation energy and the dissociation process.

Nevertheless, the above observations could be attributed to the ionization followed by dissociation mechanism, where the later process takes place in the vibrationally hot states of the ground electronic state of molecular ions (X), the excited electronic states of the $(P^+)^* \bar{A}$ (~ 12 eV) and \bar{B} (~ 13 eV)), and/or to the Coulomb explosion from multiply charged molecular ions.^{34–36}

The abundance of the P^+ peaks can be understood within the ionization followed by dissociation scheme. Especially, for the case of $1-C_4H_9Br$, the P^+ could not be detected in the mass spectra, even for the lowest laser intensity used ($\sim 2 \times 10^{13}$ W/cm 2). The ionization potential of the alkyl bromides varies within the range $\sim 10.11-10.29$ eV. The absorption of nine (1064 nm) photons, required for the molecular ionization, offers a total excitation energy of 10.48 eV. Thus, the absence of the P^+ peak from the mass spectra of $1-C_4H_9Br$ may be connected with the fact that this excitation energy is above the lower dissociation channel above ionization, which opens at ~ 10.20 eV.³⁶ For the C_2H_5Br and the $1-C_3H_7Br$ molecules, the corresponding dissociation channels open at 11.21 and 10.55 eV, respectively [NIST]. Therefore, for the later two molecules the fragmentation of their P^+ requires the absorption of additional photons, i.e., higher laser intensity. Obviously, the above approach is conceivable in an ionization followed by dissociation process.

Apart from the detection of the P^+ , the ionization/dissociation process can be clarified by comparing the experimental values of the fragments kinetic energies with those reported in recent publications. It is known that the photodissociation of the alkyl bromides, under laser irradiation at 267 nm (4.6 eV), leads to the production of Br fragments with kinetic energies ~ 0.8 eV.^{30,32} By taking into account that the four-photon absorption at 1064 nm offers approximately the same excitation energy, the experimental values for the kinetic energies of Br^+ can be used as a criterion for the ionization/dissociation process. In addition, the kinetic energies of the Br fragments, coming from the dissociation of excited states of the $(P^+)^*$, depend on the

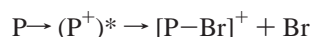
TABLE 2: Kinetic Energies of the Br^+ , Br^{2+} , and $[\text{P}-\text{Br}]^+$ of the Alkyl Bromide Fragments at the Intensity of $9.0 \times 10^{13} \text{ W/cm}^2$

kinetic energy (eV)	Br^+_{out}	Br^+_{mid}	$\text{Br}^{2+}_{\text{out}}$	$\text{Br}^{2+}_{\text{mid}}$	$[\text{P}-\text{Br}]^+_{\text{out}}$	$[\text{P}-\text{Br}]^+_{\text{mid}}$
$\text{C}_2\text{H}_5\text{Br}$	1.0 ± 0.1	0.11 ± 0.02	2.0 ± 0.2	0.13 ± 0.02	2.9 ± 0.1	0.13 ± 0.02
$1-\text{C}_3\text{H}_7\text{Br}$	1.2 ± 0.2	0.12 ± 0.02	3.6 ± 0.3	0.12 ± 0.02	2.2 ± 0.2	0.11 ± 0.02
$1-\text{C}_4\text{H}_9\text{Br}$	1.4 ± 0.2	0.11 ± 0.02	3.9 ± 0.3	0.12 ± 0.02		

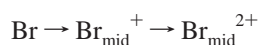
exact state from which they originate and they are known to vary in the range of ~ 0.1 – 0.3 eV.^{36–38}

The estimated experimental kinetic energy values for the $[\text{P}-\text{Br}]^+$, Br^+ , and Br^{2+} ions are presented in Table 2. The corresponding peaks exhibit a complicated peak profile, consisting of two pairs of backward and forward components, which have been attributed to different dissociation channels according to their dependence on the laser polarization. The only exception is the $[\text{P}-\text{Br}]^+$ in the $1-\text{C}_4\text{H}_9\text{Br}$ mass spectra, which is recorded as a single peak profile (Figure 2), in agreement with our earlier interpretation of the absence of the $1-\text{C}_4\text{H}_9\text{Br}$ parent ion, since its fragmentation at this energy level leaves the C_4H_9^+ with very low excess energy.

The middle pair of Br^+ components (Br^+_{mid}) corresponds to ions generated from dissociation processes producing low kinetic energy fragments (~ 0.1 eV). The values of the kinetic energies are close to those expected from an ionization followed by dissociation process, while they are clearly smaller than those expected from a dissociation-followed-by-ionization-process via the intermediate, dissociative A state. Thus, the kinetic energy values of the ions contributing to these peak components imply that molecular ionization precedes fragmentation, i.e.



In a later step, the Br fragments are ionized by the same laser pulse, resulting in the Br^+_{mid} production. Furthermore, the middle pair of Br^{2+} peak component ($\text{Br}^{2+}_{\text{mid}}$) is produced via a sequential mechanism

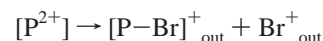


This conclusion is based on the fact that: the Br^+_{mid} and $\text{Br}^{2+}_{\text{mid}}$ ions were found to have the same kinetic energies; the laser intensity threshold for the $\text{Br}^{2+}_{\text{mid}}$ production is just above the saturation intensity of the Br^+_{mid} signal (the intensity dependence of the Br^+_{mid} , $\text{Br}^{2+}_{\text{mid}}$ signals is not presented here); the Br^+_{mid} and $\text{Br}^{2+}_{\text{mid}}$ ions exhibit the same, within the range of the experimental errors, angular distributions.

The angular distributions for the $\text{C}_2\text{H}_5\text{Br}$ fragments at the intensity of $1 \times 10^{14} \text{ W/cm}^2$ are presented in Figure 4. The same features have been observed in the angular distributions of the other alkyl bromides studied. The close resemblance between the Br^+_{mid} and the $[\text{P}-\text{Br}]^+_{\text{mid}}$ angular distributions implies that these fragments are generated mainly from the same dissociation route.

On the other hand, the values of the kinetic energies of the ions contributing to the outer pair of components of the Br^+ (Br^+_{out}) peak, imply that these fragments are generated by a Coulomb explosion process. These values are higher than the ones expected on the basis of a simple bond fragmentation process, even for the case of a nonstatistical dissociation. The resemblance of the Br^+_{out} distribution with that of $[\text{P}-\text{Br}]^+_{\text{out}}$ (Figure 4) confirms once again the proposed discrimination of the ion signal to Br^+_{mid} and Br^+_{out} components. Moreover, the average kinetic energies of these fragments are in agreement with the conservation of momentum provided that their origin is the same dissociation channel. The above results support the

conclusion that the main dissociation channel is the cleavage of the C–Br bond, i.e.



Nevertheless, minor contribution from different Coulomb explosion channels producing Br^+_{out} ions cannot be excluded. The estimated value for the critical bond length was found $R_{\text{cr}} (\text{\AA}) = 3.8 \pm 0.2$, which is about twice the bond length C–Br in the equilibrium ($R_{\text{eq}} (\text{\AA}) = 1.94$).

As far as the $\text{Br}^{2+}_{\text{out}}$ ions are concerned, their average kinetic energy is found to be twice that of Br^+_{out} , while their angular distribution is narrower than the one of Br^+_{out} . These results indicate that the $\text{Br}^{2+}_{\text{out}}$ ions are generated from the Coulomb explosion of higher charged species $[\text{P}^{n+}]$, with $n \geq 3$. By assumption that the precursor for the $\text{Br}^{2+}_{\text{out}}$ is an unstable $[\text{P}^{3+}]$ and the dissociation channel is $[\text{P}^{3+}] \rightarrow [\text{P}-\text{Br}]^+_{\text{out}} + \text{Br}^{2+}_{\text{out}}$, the corresponding critical bond length can be estimated by the following equations

$$E[\text{P}^{(n+m)+}] (\text{eV}) = \left(1 + \frac{m(\text{X})}{m(\text{P}-\text{X})}\right) E_{\text{kin}} \text{X}^{n+} (\text{eV}) \quad (3)$$

$$E[\text{P}^{(n+m)+}] (\text{eV}) = 14.4 \frac{nm}{R_{\text{cr}} (\text{\AA})} \quad (4)$$

where n and m are the charge multiplicities of the Br and $[\text{P}-\text{Br}]$ fragment ions.

Thus, when the Coulomb explosion is taking place within a $[\text{P}^{3+}]$, the estimated value for R_{cr} is $3.8 \pm 0.3 \text{\AA}$, which is the same as that for the $[\text{P}^{2+}]$ ion. Therefore, the above hypothesis leads to a result, which is consistent with the accumulated knowledge of the enhanced ionization of diatomic molecules, i.e., that the critical molecular bond length is the same for all the Coulomb explosion channels.¹¹ However, there have been some reports concerning the multiple ionization of diatomic and polyatomic molecules that contradict with the above physical picture. In particular, the multiple ionization of the strongly bound N_2O ³⁹ and C_6H_6 ⁴⁰ molecules, under strong femtosecond laser irradiation, was found to take place at the equilibrium distance of their neutral structure. The same was also concluded by Tzallas et al. for the higher-charged transient species of certain aromatic molecules, under similar conditions of irradiation.⁴¹ On the other hand, for the case of the N_2 ⁴² and NO ,⁴³ molecules it was concluded that the doubly charged species are formed at the equilibrium distance, while the higher-charged states were formed at elongated molecular bond lengths.

The experimental findings for the $1-\text{C}_3\text{H}_7\text{Br}$ are quite similar with those obtained for the $\text{C}_2\text{H}_5\text{Br}$. Both the kinetic energies of these fragments and the resemblance of their angular distributions (not presented here) have verified the proposed Coulomb explosion channel of a $[\text{P}^{2+}]$ precursor to Br^+_{out} and $[\text{P}-\text{Br}]^+_{\text{out}}$ for the $1-\text{C}_3\text{H}_7\text{Br}$ case. Moreover, the critical distance is found to be $R_{\text{cr}} (\text{\AA}) = 4.2 \pm 0.3$, which is in a reasonable agreement with the corresponding value for ethyl bromide, since the C–Br bond length in equilibrium is essentially the same for all the alkyl bromides studied. For the case of $1-\text{C}_4\text{H}_9\text{Br}$, the $[\text{P}-\text{Br}]^+_{\text{out}}$ could not be detected. The estimated R_{cr} value,

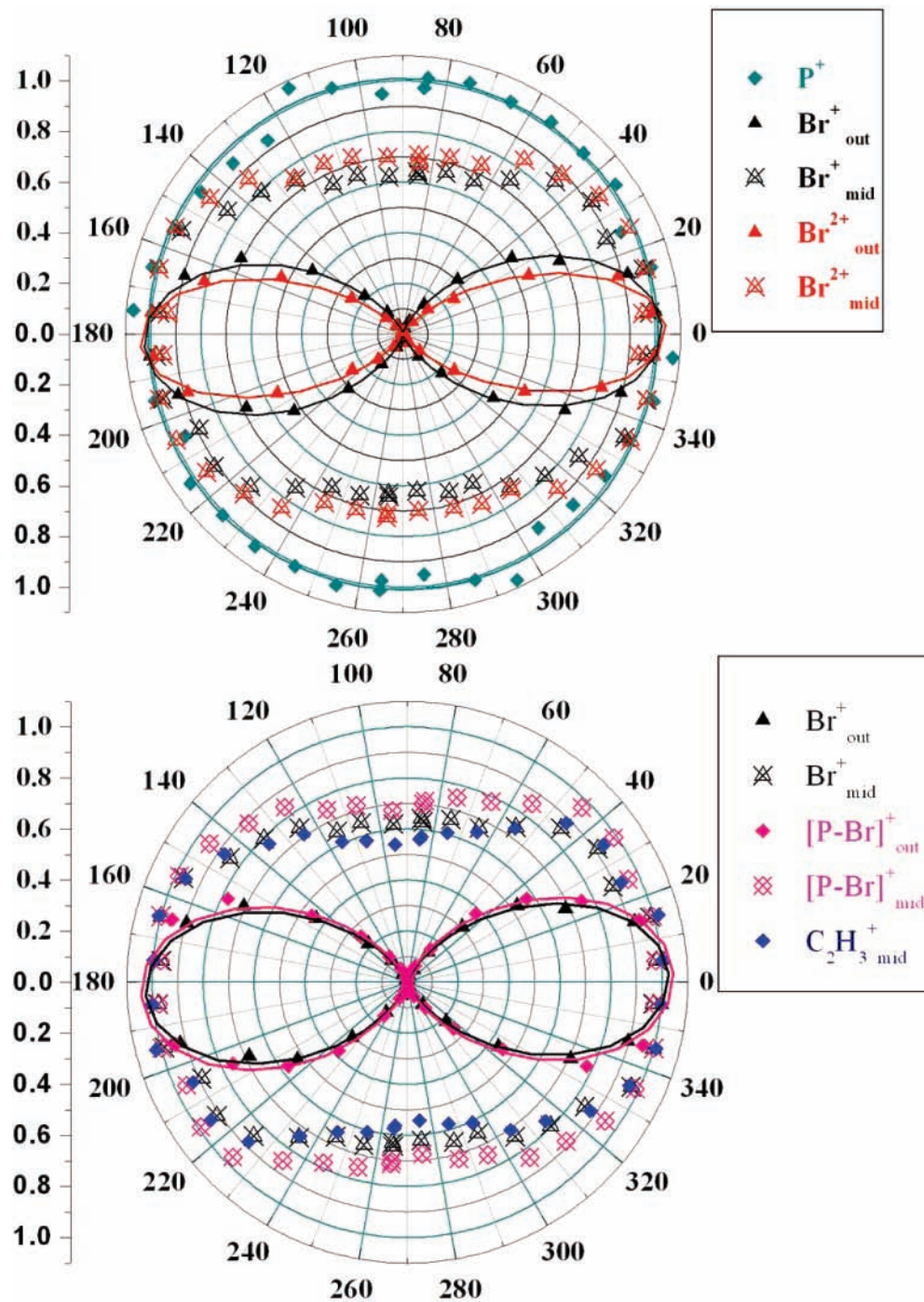


Figure 4. Angular distributions of the ethyl bromide fragment ions recorded at the intensity of 1.0×10^{14} W/cm². The data presented for the Br⁺ and Br²⁺ distributions correspond to the Br₈₁ isotope. The same distributions were also recorded for the case of Br₇₉.

based on the kinetic energies of the Br⁺_{out}, is found to be the same as before. In other words, the comparative analysis of the different kinetic energies of the Br⁺_{out} ions of the alkyl bromides indicates similar ionization processes for the three molecules.

However, some quantitative variations can be observed in the average kinetic energy values of the Br²⁺_{out} ions for the three alkyl bromides. The measured energies increase dramatically as the size of the alkyl chain increases. For 1-C₃H₇Br and 1-C₄H₉Br, the E_{kin} for Br²⁺_{out} ions are almost three times the E_{kin} of Br⁺_{out}. This observation is a clear evidence that the Br²⁺_{out} ions are produced via a Coulomb explosion within higher charged transient parent ions ([P^{*n*+}], $n \geq 3$) in comparison with the Br⁺_{out} ions. Furthermore, it could also imply a contribution to the production of Br²⁺_{out} from higher charged parent ions

for the molecules with longer alkyl chain in comparison to the ethyl bromide. However, the exact determination of the multiplicity of the Br²⁺_{out} precursors is a rather difficult task for the case of polyatomic molecules. Thus, at this point it is fraught with danger to deduce any conclusions about the possible dependence of multiple ionization on the size of the alkyl chain.

As an alternative, we chose to use the relative abundance of the (Br²⁺/Br⁺) ions for the two different ionization mechanisms. Having established that the Br²⁺_{out} and the Br⁺_{out} ions have precursors with different charged states, the (Br²⁺/Br⁺)_{out} ratio is an indirect way to measure the relative abundance of the higher charged molecular ions produced, over those of lower charged states. The ratios of (Br²⁺/Br⁺) for both Br_{mid} and Br_{out} mechanisms are depicted in Figure 5.

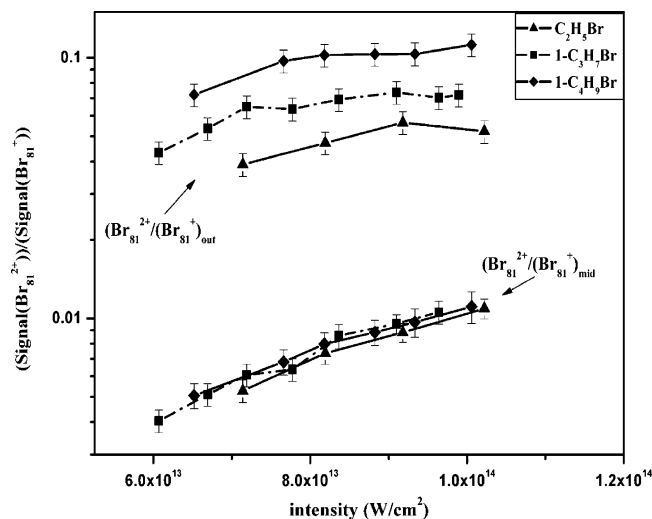


Figure 5. Dependence of the ratio $\text{Br}^{2+}/\text{Br}^+$ on the laser intensity for the alkyl bromides under study. The data presented correspond to the Br_{81} isotope.

TABLE 3: Intensity Thresholds for the Production of the Br^{n+} , $n = 1-2$, Fragments under Picosecond Laser Irradiation

intensity thresholds (10^{13} W/cm 2)	$\text{Br}^{2+}_{\text{out}}$	$\text{Br}^{2+}_{\text{mid}}$	Br^+
$\text{C}_2\text{H}_5\text{Br}$	4.6 ± 0.2	5.0 ± 0.2	$\leq 2.3 \pm 0.2$
$1\text{-C}_3\text{H}_7\text{Br}$	4.6 ± 0.2	5.0 ± 0.2	
$1\text{-C}_4\text{H}_9\text{Br}$	4.3 ± 0.2	5.0 ± 0.3	

The comparison of the $(\text{Br}^{2+}/\text{Br}^+)_{\text{out}}$ ratio for the three molecules indicates that at the same laser intensities the enhanced ionization is more efficient for the molecules with longer alkyl chain, despite the fact that they consist of the same atoms and have similar vertical ionization potentials. Thus, at the same conditions of laser irradiation the recorded ratio for the $1\text{-C}_4\text{H}_9\text{Br}$ is twice that of the $\text{C}_2\text{H}_5\text{Br}$ and 1.4 times that of the $1\text{-C}_3\text{H}_7\text{Br}$.

On the contrary, the $(\text{Br}^{2+}/\text{Br}^+)_{\text{mid}}$ is the same for all the studied alkyl bromides, within the range of experimental errors, at all laser intensities. The $\text{Br}^{2+}_{\text{mid}}$ are found to originate from further ionization of either Br^+_{mid} and/or neutral Br but not directly from molecular ions, i.e., the plot for the $(\text{Br}^{2+}/\text{Br}^+)_{\text{mid}}$ ratio reflects the atomic ionization process for species (atoms) released from the molecular dissociation. Therefore, in accordance with the experimental results, a dependence of this ratio on the size of the molecular chain is not anticipated. Nevertheless, the variation of these two ratios with respect to the alkyl chain length underlines the importance of the $(\text{Br}^{2+}/\text{Br}^+)_{\text{out}}$ ratio as a measure of the dependence of the laser/molecule coupling on molecular size.

The intensity thresholds of the alkyl bromide fragments are presented in Table 3. The ones for the $\text{Br}^{2+}_{\text{mid}}$ fragments are found to be especially independent of the size of the molecular chain. This also stands for the thresholds of the $\text{Br}^{2+}_{\text{out}}$ fragments within the range of experimental errors. The comparison of the thresholds of the $\text{Br}^{2+}_{\text{mid}}$ and $\text{Br}^{2+}_{\text{out}}$ ions indicates (especially for the case of $1\text{-C}_4\text{H}_9\text{Br}$) that the production of doubly charged Br^{2+} directly from the fragmentation of highly charged molecular ions is achieved at lower laser intensity than that needed for sequential ionization of atomic fragments released from neutral states. Moreover, the abundance of $\text{Br}^{2+}_{\text{out}}$ is found to be much higher than that of $\text{Br}^{2+}_{\text{mid}}$. In particular, for the case of ethyl bromide the ion signal for $\text{Br}^{2+}_{\text{out}}$ is 3.5 times that of $\text{Br}^{2+}_{\text{mid}}$, while in the case of 1-butyl bromide the corresponding

value is 7. These results are in accordance with those reported by Normand et al. for the multiple ionization of I_2 under strong femtosecond laser irradiation⁴⁴ and with the predictions of the theoretical models describing the enhanced ionization phenomena.

The Alkyl Chlorides. The mass spectra of the alkyl chlorides present some common features with those recorded for the alkyl iodide and alkyl bromide molecules. Once again, the abundance of the P^+ and the $[\text{P}-\text{Cl}]^+$ ions decrease in the mass spectra of the longer chain molecules. For the case of $1\text{-C}_4\text{H}_9\text{Cl}$, the P^+ peak could not be detected even for the lowest irradiation used in the present work, in contrast to the mass spectra induced by electron ionization impact, where a small P^+ peak has been reported [NIST].⁴⁵ The extended fragmentation could be attributed to a ionization followed by dissociation mechanism, provided that the ionization is an MPI process. In that case, the absorption of 10 photons at 1064 nm is required for the ionization of all these molecules, since their ionization potential varies in the range of 10.49–10.98 eV. Thus, the excitation to ionic states leads to the molecular fragmentation, according to the various dissociation channels reported previously. Especially for the case of ethyl chloride the contribution of the ladder climbing process can be verified by the detection of the $\text{CH}_2\text{-Cl}^+$, which is known to be formed in the ionic manifold [NIST].

However, the recorded molecular and atomic fragment ions can be produced by a-fragmentation-followed-by-ionization process, which takes place within the 35 ps laser pulse duration. This process can be realized through the dissociative A band of the alkyl chlorides or higher excited states of the neutral molecules. Unfortunately, the literature on the photodissociation dynamics of the alkyl chlorides and the produced fragmentation kinetic energies is rather limited in comparison to the available data for the alkyl bromide molecules. Thus, we cannot use the experimental values of the fragments' kinetic energy as a criterion for the discrimination between the ladder switching and the ladder climbing processes.

Nevertheless, following the same methodology as for the alkyl bromides, the contribution of different dissociation channels in the production of the Cl^+ , Cl^{2+} , and $[\text{P}-\text{Cl}]^+$ ions can be identified, according to their dependence on the laser polarization. The angular distributions for the case of ethyl chloride are depicted in Figure 6, while similar distributions are recorded for the rest of the molecules.

The kinetic energy values of the Cl^+ , Cl^{2+} , and $[\text{P}-\text{Cl}]^+$ ions recorded at the intensity of $\sim 8.0 \times 10^{13}$ W/cm 2 are presented in Table 4. The analysis of the kinetic energy values leads to similar conclusions with those reported for the corresponding alkyl bromide molecules.

The values of the kinetic energies for the Cl^+_{mid} and $\text{Cl}^{2+}_{\text{mid}}$ peaks indicate that these are not generated from a Coulomb explosion process. Moreover, the fact that the kinetic energies and the angular distributions of these ions are found to be the same, within the experimental errors, implies that they are released from a common dissociation process of neutral or single charged molecular ions, taking place within the laser pulse duration. In both cases the dissociation is more likely to produce the neutral atomic Cl fragment, which is sequentially ionized to a final ionization stage. It seems that, the sequential ionization process



is more likely to occur, since the laser intensity threshold for the $\text{Cl}^{2+}_{\text{mid}}$ (8.3×10^{13} W/cm 2) production is just above the saturation intensity for the Cl^+_{mid} .

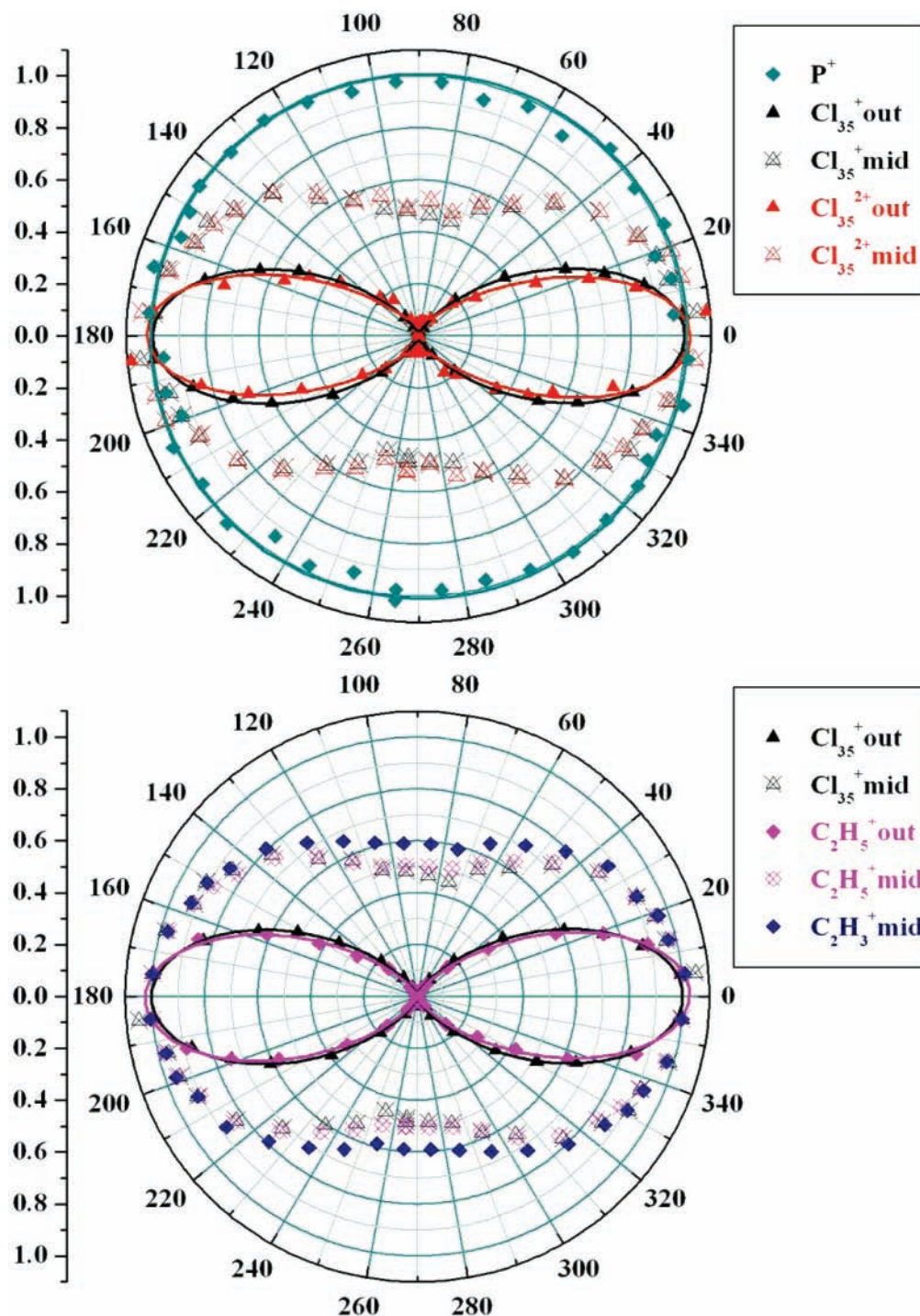


Figure 6. Angular distributions of the ethyl chloride fragment ions recorded at the intensity of 1.0×10^{14} W/cm². The data presented for the Cl⁺ and Cl²⁺ distributions correspond to the Cl₃₅ isotope. The same distributions were also recorded for the case of Cl₃₇.

TABLE 4: Kinetic Energies of the Cl⁺, Cl²⁺, and [P–Cl]⁺ of the Alkyl Bromide Fragments at the Intensity of 9.0×10^{13} W/cm²

kinetic energy (eV)	Cl ⁺ _{out}	Cl ⁺ _{mid}	Cl ²⁺ _{out}	Cl ²⁺ _{mid}	[P–Cl] ⁺ _{out}	[P–Cl] ⁺ _{mid}
C ₂ H ₅ Cl	1.9 ± 0.2	0.23 ± 0.03	3.9 ± 0.2	0.19 ± 0.03	2.2 ± 0.1	0.24 ± 0.03
1-C ₃ H ₇ Cl	2.3 ± 0.2	0.24 ± 0.03	6.8 ± 0.3	0.22 ± 0.03		
1-C ₄ H ₉ Cl	2.7 ± 0.3	0.38 ± 0.04	8.1 ± 0.7	0.34 ± 0.04		

The kinetic energies values of the Cl⁺_{out} and Cl²⁺_{out} ions are much higher than that expected from typical molecular dissociation processes. These results imply that the ions, mentioned above, originate from a Coulomb explosion process within multiply charged parent ions.

For the case of ethyl chloride, the production of the Cl⁺_{out} and [P–Cl]⁺_{out} ions is attributed to the Coulomb explosion of

[P²⁺]. This conclusion is supported by their common angular distributions (see Figure 6) and also by the fact that the ratio of their average kinetic energy values is equal to the inverse ratio of their masses. The R_{cr} value of the C–Cl bond is found to be R_{cr} (Å) = 3.5 ± 0.2 , which is approximately twice the bond length at equilibrium (1.74 Å). The E_{kin} of Cl²⁺_{out} ions is twice the E_{kin} of Cl⁺_{out}, implying that the Cl²⁺_{out} are produced by

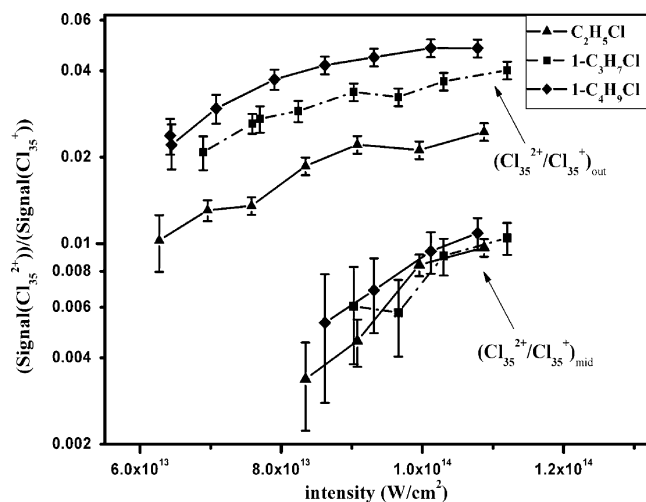


Figure 7. Dependence of the ratio $\text{Cl}^{2+}/\text{Cl}^+$ on the laser intensity for the alkyl chlorides under study. The data presented correspond to the Cl_{35} isotope.

Coulomb explosion of higher charged parent ions ($[\text{P}^{n+}]$, $n \geq 3$). By assumption that the precursor of $\text{Cl}^{2+}_{\text{out}}$ is $[\text{P}^{3+}]$, the critical bond length is found to be $R_{\text{cr}} (\text{\AA}) = 3.4 \pm 0.2$, i.e., the same as that of $[\text{P}^{2+}]$. The above results are in accordance with those found for the case of the ethyl bromide.

As far as the other alkyl chlorides are concerned the kinetic energies of the Cl^+_{out} and $\text{Cl}^{2+}_{\text{out}}$ ions imply that they are produced via Coulomb explosion process of multiply charged parent ions. Since the corresponding $[\text{P}-\text{Cl}]^+_{\text{out}}$ peaks are too small for the precise determination of their kinetic energies and angular distributions, no experimental evidence is available for the determination of the Cl^+_{out} precursor. Nevertheless, by making the reasonable assumption that the Cl^+_{out} ions originate from the Coulomb explosion of transient doubly charged molecular ions ($[\text{P}^{2+}]$), the critical C–Cl bond length can be estimated by using the eqs 1 and 2. For both the 1- $\text{C}_3\text{H}_7\text{Cl}$ and the 1- $\text{C}_4\text{H}_9\text{Cl}$ molecules, the estimated values of the R_{cr} are found to be the same as that for the ethyl chloride.

On the other hand, the average kinetic energies of the $\text{Cl}^{2+}_{\text{out}}$ fragments are found to be higher than those of Cl^+_{out} and therefore the precursor of the former ion should be molecular ions of higher charged states than those of the later. The exact determination of the multiplicity of the fragment ions' precursors is rather difficult, as in the case of alkyl bromides, and no safe conclusions, based on these observations, can be reached about the dependence of multiple ionization on the size of the alkyl chain.

As stated above for the alkyl bromides, the comparison of the ratios $(\text{Cl}^{2+}/\text{Cl}^+)_{\text{out}}$ for the three alkyl chlorides can be used as a criterion for the relative efficiency of the multiple ionization of these molecules. These ratios are depicted in Figure 7. From the comparison of these ratios it is concluded that, within the range of the laser intensities ($6 \times 10^{13} - 1.2 \times 10^{14}$) W/cm^2 , the enhanced multiple ionization is more efficient for molecules with longer alkyl chain. In particular, at the intensity of 1.0×10^{14} W/cm^2 , the recorded ratio for the 1- $\text{C}_4\text{H}_9\text{Cl}$ is 2.3 times that of $\text{C}_2\text{H}_5\text{Cl}$ and 1.4 times that of 1- $\text{C}_3\text{H}_7\text{Cl}$. At the same time, the $(\text{Cl}^{2+}/\text{Cl}^+)_{\text{mid}}$ ratio has similar value for all the alkyl chlorides studied, within the range of experimental errors at all laser intensities. The $\text{Cl}^{2+}_{\text{mid}}$ are found to originate from further ionization of either Cl^+_{mid} and/or neutral Cl but not directly from multiply charged molecular ions. Thus, taking into account that the laser intensity threshold for the $\text{Cl}^{2+}_{\text{mid}}$ is far above the saturation intensity of the Cl^+_{mid} yield, the independence of their

TABLE 5: Intensity Thresholds for the Production of the Cl^{n+} , $n = 1-2$, Fragments under Picosecond Laser Irradiation

intensity thresholds (10^{13} W/cm^2)	$\text{Cl}^{2+}_{\text{out}}$	$\text{Cl}^{2+}_{\text{mid}}$	Cl^+
$\text{C}_2\text{H}_5\text{Cl}$	5.9 ± 0.2	8.3 ± 0.2	2.8 ± 0.2
1- $\text{C}_3\text{H}_7\text{Cl}$	5.5 ± 0.2	8.4 ± 0.2	2.8 ± 0.2
1- $\text{C}_4\text{H}_9\text{Cl}$	4.7 ± 0.2	8.3 ± 0.2	2.6 ± 0.2

ratio on the size of the molecular chain is anticipated. This interpretation is in accordance with the fact that the laser intensity thresholds of the $\text{Cl}^{2+}_{\text{mid}}$ ions are also independent of the molecular size. The intensity thresholds for the production of the Cl^+ and Cl^{2+} ions are presented in Table 5.

From this table, it is clear that the laser intensity threshold values for the $\text{Cl}^{2+}_{\text{out}}$ are found to decrease as the size of the alkyl chain increases. This result is interesting, since it is a direct experimental evidence of the enhanced multiple ionization rate of the alkyl chlorides as the size of the molecular chain increases. It should be mentioned that for the alkyl iodide and alkyl bromide molecules the differences in the laser intensity thresholds for their halogen ions as the molecular size increases are very small and comparable to the experimental errors. Thus, only for the case of the alkyl chloride molecules was it possible to observe a clear trend for the intensity thresholds of their $\text{Cl}^{2+}_{\text{out}}$ fragments as the size of the alkyl chain increases. This observation indicates that the differentiation of the ionization rates for the same increment of the molecular chain is more effective for the alkyl chloride in comparison to that for the rest alkyl halides, under study. This result is conceivable by taking into account that the C–Cl bond is shorter than the corresponding C–X, X = Br, I, and its polarizability is smaller. Therefore, the total molecular length and the polarizability of the alkyl chlorides are more dramatically affected by the particular increment of the molecular chain than those for the other alkyl halides.

Moreover, the comparison of the thresholds for the $\text{Cl}^{2+}_{\text{out}}$ and $\text{Cl}^{2+}_{\text{mid}}$ ions imply that the production of the Cl^{2+} originating from the direct dissociation of an unstable parent ion $[\text{P}^{n+}]$, with $n \geq 3$, requires lower laser intensity in comparison to a process that involves atomic ionization. Finally, the production of Cl^{2+} generated from fragmentation of multiply charged molecular ions, is more efficient than that arising from the ionization of atomic fragments, as we can see from the relative abundance of ions contributing to the $\text{Cl}^{2+}_{\text{out}}$ and $\text{Cl}^{2+}_{\text{mid}}$ peak components. For instance, in the case of $\text{C}_2\text{H}_5\text{Cl}$, the abundance of the $\text{Cl}^{2+}_{\text{out}}$ is twice that of $\text{Cl}^{2+}_{\text{mid}}$, while in the case of 1- $\text{C}_4\text{H}_9\text{Cl}$ the corresponding value is 8.6.

Conclusions

The mass spectra of certain alkyl halides induced by a strong 35 ps laser have been recorded. The studied molecules are the following: $\text{C}_2\text{H}_5\text{X}$, 1- $\text{C}_3\text{H}_7\text{X}$, 1- $\text{C}_4\text{H}_9\text{X}$, where X = I, Br, Cl. The laser wavelength was 1064 nm, and the intensity range was $1 \times 10^{13} - 1.2 \times 10^{14}$ W/cm^2 . Under these laser irradiation conditions multielectron dissociative ionization (MEDI) of the studied molecules have been achieved. The confirmation of MEDI is based on the estimated values for the kinetic energies of the released fragments and their dependence on laser intensity and polarization. This conclusion is in agreement with that previously reported for the case of alkyl iodides.^{18,26}

The recorded ion peaks reveal a complex structure which accounts for ion production from different dissociation channels and their ejection toward or backward the detector ("backward"/"forward" components). The ion peaks that correspond to the

halogen ions and also, in some cases, to the $[P-X]$ ions, are found to consist of two pairs of components, the outer (labeled as out) and the middle one (labeled as mid). On the basis of the angular distribution of the fragment ions (especially each of these pairs of components), the dependence on laser intensity and their kinetic energies, different dissociation channels of unstable multiply charged parent ions have been identified.

Thus, for the particular molecules where the $[P-X]_{\text{out}}^+$ ion has been recorded the Coulomb explosion of the corresponding precursors ($[P^{2+}]$) is found to take place at critical elongated C–X bond lengths, which is estimated to be twice that of the equilibrium values. These results are in agreement with the predictions of the enhanced multiple ionization theoretical models^{11–13} and with the experimental results on various diatomic molecules. As it is known, the bond elongation prior to the molecular dissociation accounts for the observed lower kinetic energies of the released ion fragments than those expected if they were generated from the ground state geometry. Thus, the observed increase of the kinetic energy values for the halogen ions (X_{out}^+ , X_{out}^{2+} , X_{mid}^+ , X_{mid}^{2+}) originating from precursors that have the same alkyl part but smaller C–X bond length ($C-I > C-Br > C-Cl$) is reasonable, along with the fact that the lighter fragments ($m_{Cl} < m_{Br} < m_I$) are released with higher kinetic energy due to momentum conservation. Moreover, it is expected that the ratios of the kinetic energy values of the different halogen ions (i.e., $Br_{\text{out}}^+/Cl_{\text{out}}^+$, $Br_{\text{out}}^{2+}/Cl_{\text{out}}^{2+}$, $Br_{\text{mid}}^+/Cl_{\text{mid}}^+$, $Br_{\text{mid}}^{2+}/Cl_{\text{mid}}^{2+}$) should remain almost constant for the molecules with the same alkyl chain length. This is verified, within the experimental errors, for all the molecules under study.

As far as the dependence of the multiple ionization rates on the size of the molecular chain is concerned, this has been investigated by comparing the ratio of the doubly charged halogen ions to the singly charged ones, provided that both of these ions are released from multiply charged parent ions. This approach is preferred to the comparison based on the total ion signal because of the possible contribution from the ladder switching processes and the fact that the molecules chosen have only one halogen atom in their skeleton, namely, a one-to-one correspondence between X ions and parent molecules can be established. Thus, the ratios $(X^{2+}/X^+)_{\text{out}}$ are found to vary with the length of alkyl chain, while the ratios $(X^{2+}/X^+)_{\text{mid}}$ have similar values for molecules with different sizes. Since the X_{mid}^{2+} and X_{mid}^+ ions are generated by further ionization of neutral and/or singly charged atomic fragments released from molecular dissociation, their ratios reflect the dependence of an atomic ionization process on laser intensity, and this is why they are independent of the molecular size. On the contrary, the $(X^{2+}/X^+)_{\text{out}}$ ratios are indicative for MEDI processes because it has been established that these ions are released directly from the fragmentation of multiply charged parent ions, therefore the dependence of these ratios on molecular length reflects the dependence of MEDI on molecular size.

In the present work, it is found that the $(X^{2+}/X^+)_{\text{out}}$ ratios increase as the size of the molecular chain increases for both the alkyl bromide and alkyl chloride molecules. These observations imply that the molecular coupling with the laser field increases with the molecular size, at least for the studied molecules. This conclusion was impossible to arrive at on the basis of the comparison of the relative total ion yields and on the trend of the laser threshold intensity for the appearance of the multiply charged ions. It should be mentioned that, only for Cl^{2+} generated from Coulomb explosion of $1-C_4H_9Cl$ ions, the laser intensity threshold can be used to safely arrive at a

conclusion with respect to MEDI efficiency. Of course, the trend of the Cl^{2+} intensity threshold is in agreement with the remarks made on the grounds of the dependence of the $(X^{2+}/X^+)_{\text{out}}$ ratio on size of the alkyl chain.

The fact that this trend was clearly observed only for the alkyl chloride molecules indicates that the differentiation of the ionization rates, for the same increment of the molecular chain, is more effective for these molecules than for the other alkyl halides.

The above results are clearly at variance with those reported by Hering et al.¹⁵ where the ionization rates of diatomic and triatomic molecules consisting of the same atoms were found to be approximately the same.

The relative abundances of the highly energetic Cl^{2+} and Br^{2+} ions (the X_{out}^{2+} peak components) in comparison to the low energy ones prove that these ions are produced more efficiently by the multiple molecular ionization of parent ions in comparison to ionization processes that involves atomic ionization steps. This is also in accordance with the observation that the laser intensity thresholds for the X_{out}^{2+} components are lower than those of X_{mid}^{2+} ones. This result is in agreement with the predictions of the theoretical models concerning the enhanced multiple ionization phenomena and, also, with some experimental works^{44,46} reported in the past.

Moreover, from the comparison of the laser intensity thresholds for the atomic halogen ions, it is clear that they are following the trend of the ionization potential energies (IE) for the production of these ions (the $IE(P^{n+}) < IE(Br^{n+}) < IE(Cl^{n+})$, $n \leq 3$). This is self-evident for the X_{mid}^{n+} ions (their generation have been attributed to atomic ionization processes), but the case of the X_{out}^{n+} ions is worth some further discussion because, as stated above, they are the direct product of the molecular fragmentation. It could be argued, that the lower laser intensity threshold accounts for the fact that the halogen atoms with lower IE values are forming longer C–X bonds, thus the trend of the thresholds reflects the dependence of the molecular coupling with the laser field on the molecular size. Nevertheless, this argument is not supported by the intensity threshold values for halogen ions generated from molecules with different molecular size; for instance, the threshold for the Br_{out}^{2+} released from C_2H_5Br is lower than that of Cl_{out}^{2+} ejected from the longer $1-C_3H_7Cl$. On the contrary, if the approach based on the trend of the atomic IE values is adapted for the (molecular fragments) X_{out}^{n+} ions too, then the experimentally observed laser intensity thresholds are readily understood. Obviously, this approach implies that atoms in a molecule should not be treated simply as “a noumenon in the sense of Kant”.⁴⁷

Acknowledgment. We would like to express our thanks to the Central Laser Facility of the University of Ioannina for their facilities and their assistance. This research was funded by the program “Heraklitos” of the Operational Program for Education and Initial Vocational Training of the Hellenic Ministry of Education under the third Community Support Framework and the European Social Fund.

References and Notes

- (1) Keldysh, L. V. *Sov. Phys. JEPT* **1965**, *20*, 1307.
- (2) DeWitt, M. J.; Levis, R. J. *J. Chem. Phys.* **1998**, *108*, 7045.
- (3) DeWitt, M. J.; Levis, R. J. *J. Chem. Phys.* **1998**, *108*, 7739.
- (4) DeWitt, M. J.; Levis, R. J. *J. Chem. Phys.* **1999**, *110*, 11368.
- (5) Markevitch, A. N.; Moore, N. P.; Levis, R. J. *J. Chem. Phys.* **2001**, *267*, 131.
- (6) Hankin, S. M.; Villeneuve, D. M.; Corkum, P. B.; Rayner, M. D. *Phys. Rev. A* **2001**, *64*, 013405.

- (7) Lezius, M.; Blanchet, V.; Ivanov, M. Y.; Stolow, A. *J. Chem. Phys.* **2002**, *117*, 1575.
- (8) Markevitch, A. N.; Smith, S. M.; Romanov, D. A.; Schlegel, B. H.; Ivanov, M. Y.; Levis, R. J. *Phys. Rev. A* **2003**, *68*, 011402.
- (9) Markevitch, A. N.; Romanov, D. A.; Smith, S. M.; Schlegel, B. H.; Ivanov, M. Y.; Levis, R. J. *Phys. Rev. A* **2004**, *69*, 013401.
- (10) Kitzler, M.; Zanghellini, J.; Jungreuthmayer, Ch; Smits, M.; Scrinzi, A.; Brabec, T. *Phys. Rev. A* **2004**, *70*, 041401.
- (11) Posthumus, J. H. *Rep. Prog. Phys.* **2004**, *67*, 623.
- (12) Seideman, T.; Ivanov, M. Yu.; Corkum, P. B. *Phys. Rev. Lett.* **1995**, *75*, 2819.
- (13) Posthumus, J. H.; Frasinski, L. J.; Giles, A. J.; Codling, K. *J. Phys. B: At. Mol. Opt. Phys.* **1995**, *28*, L349.
- (14) Schröder, H.; Uiterwaal, C. J. G. J.; Kompa, K. L. *Laser Phys.* **2000**, *7*, 749.
- (15) Hering, Ph.; Cornaggia, C. *Phys. Rev. A* **1998**, *57*, 4572.
- (16) Hatherly, P. A.; Frasinski, L. J.; Codling, K.; Barr, J. R. M. *Chem. Phys. Lett.* **1988**, *149*, 477.
- (17) Kosmidis, C.; Siozos, P.; Kaziannis, S.; Robson, L.; Ledingham, K. W. D.; McKenna, P.; Jaroszynski, D. A. *J. Phys. Chem. A* **2005**, *109*, 1279.
- (18) Siozos, P.; Kaziannis, S.; Kosmidis, C.; Lyras, A. *Int. J. Mass. Spectr.* **2005**, *243*, 189.
- (19) August, S.; Meyerhofer, D.; Strickland, D.; Chin, S. L. *J. Opt. Soc. Am. B* **1991**, *8*, 858.
- (20) DeWitt, M. J.; Peters, D. W.; Levis, R. J. *J. Chem. Phys.* **1997**, *218*, 211.
- (21) Kosmidis, C.; Tzallas, P.; Ledingham, K. W. D.; McCanny, T.; Singhal, R. P.; Taday, P. F.; Langley, A. J. *J. Phys. Chem. A* **1999**, *103*, 6950.
- (22) Robson, L.; Ledingham, K. W. D.; Tasker, A. D.; McKenna, P.; McCanny, T.; Kosmidis, C.; Jaroszynski, D. A.; Jones, D. R.; Issac, R. C.; Jamieson, S. *Chem. Phys. Lett.* **2002**, *360*, 382.
- (23) Fuß, W.; Schmid, W. E.; Trushin, S. A. *J. Chem. Phys.* **2000**, *112*, 8347.
- (24) Trushin, S. A.; Fuß, W.; Schmid, W. E. *J. Phys. B* **2004**, *37*, 3987.
- (25) Nakashima, N.; Shimizu, S.; Yatsuhashi, T.; Sakabe, S.; Izawa, Y. *J. Photochem. Photobiol., C* **2000**, *1*, 131.
- (26) Siozos, P.; Kaziannis, S.; Kosmidis, C. *Int. J. Mass. Spectrom.* **2003**, *225*, 249.
- (27) Graham, P.; Ledingham, K. W. D.; Singhal, R. P.; Hankin, S. M.; McCanny, T.; Fang, X.; Kosmidis, C.; Tzallas, P.; Taday, P. F.; Langley, A. J. *J. Phys. B: At. Mol. Opt. Phys.* **2001**, *34*, 4015.
- (28) Snyder, E. M.; Wei, S.; Purnell, J.; Buzza, S. A.; Castleman, A. W. *Chem. Phys. Lett.* **1996**, *248*, 1.
- (29) Mulliken, R. S. *J. Chem. Phys.* **1940**, *8*, 382.
- (30) Tang, Y.; Lei, J.; Rongshu, Z.; Zhengrong, W.; Bing, Z. *Chem. Phys. Chem.* **2005**, *6*, 2137.
- (31) Gougousi, T.; Samartzis, P. C.; Kitsopoulos, T. N. *J. Chem. Phys.* **1998**, *108*, 5742.
- (32) Zhang, S.; Wang, Y.; Tang, B.; Zheng, Q.; Zhang, B. *Chem. Phys. Lett.* **2005**, *413*, 129.
- (33) Tang, B.; Zhu, R.; Tang, Y.; Lei, J.; Bing, Z. *Chem. Phys.* **2004**, *303*, 37.
- (34) Tang, B.; Zhang, B. *Chem. Phys. Lett.* **2005**, *412*, 145.
- (35) Tang, B.; Zhang, S.; Wang, Y.; Tang, Y.; Zhang, B. *J. Chem. Phys.* **2005**, *123*, 164305.
- (36) Oliveira, M. C.; Baer, T.; Olesik, S.; Ferreira, M. A. A. *Int. J. Mass. Spectr. Ion Proc.* **1988**, *82*, 299.
- (37) Miller, B. E.; Baer, T. *Chem. Phys.* **1984**, *85*, 39.
- (38) Xu, D.; Price, R. J.; Huang, J.; Jackson, W. M. *Z. Phys. Chem.* **2001**, *215*, 253.
- (39) Graham, P.; Ledingham, K. W. D.; Singhal, R. P.; McCanny, T.; Hankin, S. M.; Fang, X.; Tzallas, P.; Kosmidis, C.; Taday, P. F.; Langley, A. J. *J. Phys. B: At. Mol. Opt. Phys.* **2000**, *33*, 3779.
- (40) Shimizu, S.; Kou, J.; Kawato, S.; Shimizu, K.; Sakabe, K.; Nakashima, N. *Chem. Phys. Lett.* **2000**, *317*, 609.
- (41) Tzallas, P.; Kosmidis, C.; Graham, P.; Ledingham, K. W. D.; McCanny, T.; Hankin, S. M.; Singhal, R. P.; Taday, P. F.; Langley, A. J. *Chem. Phys. Lett.* **2000**, *332*, 236.
- (42) Baldit, E.; Saugout, S.; Cornaggia, C. *Phys. Rev. A* **2005**, *71*, 21403.
- (43) Wu, J.; Zeng, H.; Guo, C. *Phys. Rev. A* **2006**, *74*, 31404.
- (44) Normand, D.; Schmidt, M. *Phys. Rev. A* **1996**, *53*, 1958.
- (45) Ferreira, M. A.; Cabral, C. B. J.; Oliveira, M. C.; Baer, T. *Org. Mass. Spectr.* **1993**, *28*, 1229.
- (46) Constant, E.; Stapelfeldt, H.; Corkum, P. B. *Phys. Rev. Lett.* **1996**, *76*, 4140.
- (47) Parr, R. G.; Ayers, P. W.; Nalewajski, R. F. *J. Phys. Chem. A* **2005**, *109*, 3957.